Journal of Materials Chemistry C

Accepted Manuscript

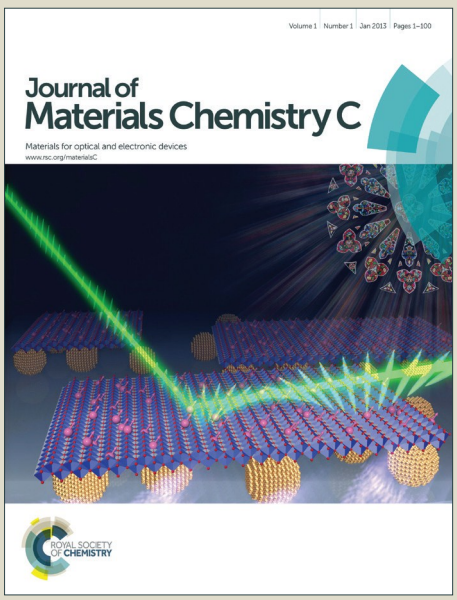

ROYAL SOCIETY OF CHEMISTRY

www.rsc.org/materialsC

Cite this: DOI: 10.1039/c0xx00000x

www.rsc.org/xxxxxx

ARTICLE TYPE

A facile formulation and excellent electromagnetic absorption of room temperature curable polyaniline nanofiber based inks

Nina Joseph [a,b], Jobin Varghese [a, b] and Mailadil Thomas Sebastian [*a, b]

A facile formulation of room temperature curable polyaniline nanofiber based absorbing ink has been developed. The polyaniline nanofiber and polyaniline nanofiber-graphite composite of 1 mm thickness exhibit average EMI shielding effectiveness of 74 and 87 dB respectively in the frequency range 8.2-18 GHz which corresponds to about 100 % of electromagnetic attenuation. Polyaniline nanofiber based screen printed layer of thickness of 50 µm showed an EMI shielding effectiveness (EMI SE) of above13 dB. Screen printed pattern formulated using graphite incorporated polyaniline nanofiber exhibits an EMI SE of about 17 dB which will prevent 98 % of electromagnetic radiation in the microwave frequency range. The dominant shielding mechanism of polyaniline nanofiber based materials is found to be absorption. The polyaniline nanofiber based screen printed patterns exhibit faster curing time along with the excellent absorption shielding properties.

1. Introduction

The problem of electromagnetic interference (EMI) results due to the rapid development of modern electronics and integrated circuits. This electromagnetic pollution is affecting all electrical and electronic systems from daily life, to military activity, space exploration as well as living environment to human beings.[1, 2] Due to sensitive high-speed circuit growth in handheld products, electrostatic discharge (ESD) has become a growing concern in the electronic industry. ESD is defined as a rapid discharge between two bodies at different potentials.[3] Hence, the modern world is looking for high-performance EMI shielding materials with good electrical and physical properties. In addition to high EMI shielding performance, thin and light weight are other important technical requirements for effective and practical EMI shielding applications especially for aircraft, aerospace, automobiles, and fast-growing next-generation flexible electronics.[4, 5]

The use of traditional metal based materials for shielding applications were limited owing to its high density, cost and corrosion.[6] EMI shielding inks with effective EMI shielding performance can solve these problems to some extent. Due to their potential low cost per surface area, mechanical flexibility and possibility of large scale processing, these inks can lead to new opportunities in the field of EMI shielding.[7, 8] Such inks can find potential for a variety EMI/RFI shielding applications, including electronic plastic housings, aerospace components and polyimide flexible circuits. Electrostatic discharge shielding (ESD) is one of the most important applications of these inks. They can reduce the ESD related problems and can lower the damage due to ESD.[9] The benefits of printed electronics include cost effectiveness, low space, low weight consumption, flexibility, environmental friendliness and robust performances. The ideal ink needs to have a combination of low cost, ease of processing and high performance. Hence, it exhibits considerable promise to offer a low-cost and high-performance solution for EMI shielding applications.[10,11] Moreover, EMI shielding inks can be easily applied to various flexible or rigid as well as shielding components.[12]

Conducting polymers are found to be exciting materials for EMI shielding applications.[13-17] Among the conducting polymers, polyaniline is known for its attractive properties such as tunable conductivity, non-corrosiveness, low density, low cost, easy synthesis method as well as good environmental and thermal stability. Hence, it has find use in a wide range of industrial and commercial applications.[14, 18-20] The good properties of conducting polymer especially polyaniline and its composites can be useful for developing effective EMI shielding materials. Such shielding materials are advantageous over traditional metal based shielding materials which are heavy and corrosive.[6, 21] The poor mechanical properties of polyaniline limit its applications to some extent.[14, 22] Hence high-performance EMI shielding materials based on polyaniline and its composites can be achieved by developing EMI shielding inks. These inks can combine the

advantages of printing technology as well as good properties of polyaniline. Polyaniline based inks can be easily printed allowing the use of reel-to-reel processing, resulting in reduced substrate handling and clean-room costs as well.[23] They can be very effective in blocking the unwanted electromagnetic radiation mainly by absorption. Absorbing ink reduces reflections and minimizes the risk from RF sources trapped inside the shielded area. Screen printing is a technique which has the advantage of simplicity, low cost, controllable thickness and uniformity of printed layer. [21] There are several reports on the EMI shielding effectiveness of screen printed carbon nanotubes, carbon black and graphite films in the frequency range of 15-1000 MHz.[21] Graphite flakes which are composed of carbon layers have been considered as another good EMI shielding material with remarkable advantages of lightweight, low cost, conductivity and easy availability.[24] Graphite flakes can also serve as a stable and underlying conductive network for the polyaniline when combining the graphite flakes and polyaniline together. Accordingly, such composite materials can have conductivity greater than graphite or polyaniline alone.[25-28] Good EMI shielding properties is expected to achieve with such composite materials. Hence, it is attractive to formulate polyaniline-graphite inks to harness these excellent properties. There are several reports on the application of screen printed polyaniline and its composite based inks for sensors, capacitors etc.[29,30] But reports on the EMI shielding properties of polyaniline ink are limited. However a report was found on EMI shielding properties of polyaniline coated on textile surface by reactive inkjet printing technique which includes separate printing of monomer and oxidant in the frequency range of 300 MHZ to 1.5 GHz.[31]

The present work focuses on the formulation and effective screen printing of inks based on polyaniline nanofiber and polyaniline nanofiber-graphite composite. The EMI shielding properties of printed ink is investigated in the frequency range of 8.2-18 GHz. The polyaniline nanofiber (P) are prepared by simple in situ polymerization route. The polyaniline nanofiber-graphite composite is obtained by adding graphite flakes (Gp) during the polymerization process. The aim of this study is to formulate absorbing ink based on polyaniline nanofiber and its composite with high shielding performance suitable for various shielding applications. To the best of our knowledge the EMI shielding properties of polyaniline nanofiber and polyaniline nanofiber-graphite composite based screen printed layer in the X and Ku band has not been reported yet.

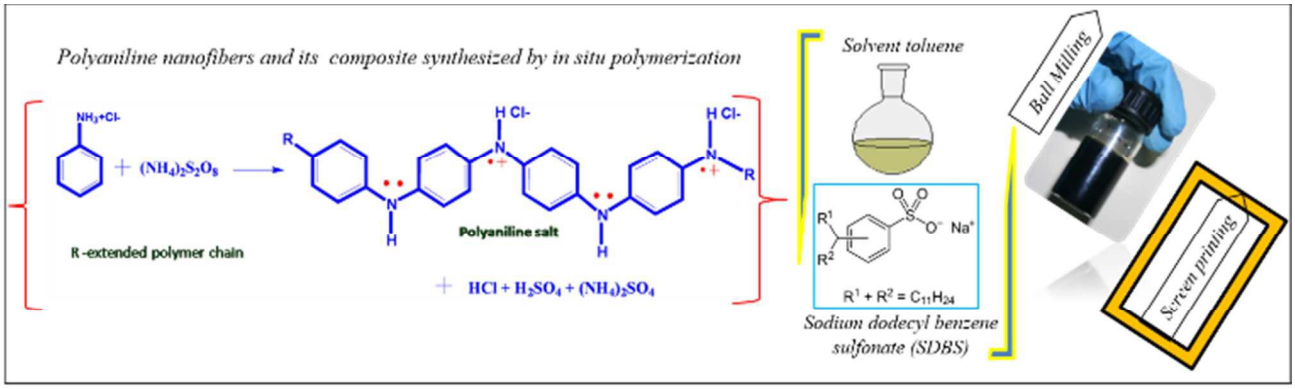

Figure 1 Formulation of polyaniline nanofiber based inks.

2. Experimental

2.1 Synthesis of polyaniline nanofiber and polyaniline nanofiber-graphite composite

The polyaniline nanofiber (P) were synthesized by in situ polymerization method. The monomer used was aniline hydrochloride (Alfa Aesar, Ward Hill, MA, USA) and oxidising agent was ammonium persulfate (APS) (Aldrich, Chemical Company, Inc., Milwaukee, WI, USA). The APS was dissolved in 1 M HCl and was added drop by drop into the aniline hydrochloride solution in 1 M HCL at room temperature. The oxidant monomer molar ratio was fixed at 1.15 and the reaction mixture was kept stable for 36 hrs. The obtained green precipitate was filtered and washed with water and methanol to remove excess acids and by-products from polymerization. The resulting powder was dried at 60 °C for 24 hrs in vacuum oven. The synthesis of polyaniline nanofiber was reported in our previous study.[32] The polyaniline nanofiber-graphite composite (GpP) was prepared in the same method as that of pure polyaniline nanofiber by taking additional component of graphite flakes (Gp). The graphite flakes of density of 2.4 g/cm^3 was bought from Carborundum Universal Ltd, Mumbai, India. The amount of filler was calculated from the desired ratio of filler relative to aniline hydrochloride. The molar ratio of aniline hydrochloride to filler (Gp) used in the present study was 4:1 i.e about 2.3 weight % (wt.%).

2.2 Ink preparation

The polyaniline nanofiber based ink was prepared by ball milling technique. The P and GpP powders were used as fillers and were synthesized by in situ polymerization route. Toluene (Aldrich chemical company, Inc, Milwaukee, WI, USA) was used as the solvent and sodium dodecyl benzene sulfonate (SDBS) (Aldrich chemical company, Inc, Milwaukee, WI, USA) as the dispersant

in the ink preparation. The filler (either P or GpP) was ball milled with toluene and SDBS for 24 hrs. After ball milling, the final composition of the ink is screen printed on 0.1 mm thick flexible BoPET (biaxially-oriented polyethylene teraphthalate (Mylar)) film, cotton cloth and white paper at a thickness of 50 µm. The schematic diagram representing the formulation of polyaniline nanofiber based ink is shown in Figure 1.

2.3 Silk screen preparation for screen printing

A silk screen of mesh size 325 tightly bounded over a metallic frame was used as the screen. Photo resist masking technique was used to develop the required printing geometry. Meshes were degreased by cleaning with acetone (Sisco Research Laboratories Pvt. Ltd., Mumbai, India) to enhance the stencil adhesion and were dried with hot air gun at 60 ^{o}C. It was then coated with solvent resistant emulsion two times on print side (substrate side) using round edges and was dried under dark light. After complete drying of emulsion, the predesigned positive image was placed over the substrate side of the screen. The emulsion surrounding the image was exposed to sunlight for few seconds. The un-cured emulsion was adhered to the portion of positive image after exposure. The un-cured emulsion on the actual print image was washed away with water and the desired print pattern was dried in air at room temperature.

2.4 Screen printing of ink

The screen printing technique created a sharp-edged image using a porous fabric and a stencil. The screen was positioned on the printable substrate and areas of the screen were blocked off with designed stencil. Ink was placed on top of the screen and was further spread evenly across the screen with a rubber squeegee. The ink passed through the open spaces in the screen onto the printable substrate below. The screen was then lifted off and can be re-used after cleaning. The P ink screen printed on BoPET substrate is designated as PI and GpP ink as GpPI.

2.5 Characterization

The phase formation of the synthesized powders was analyzed by X-ray diffraction (XRD) pattern using CuKα radiation (X'Pert PRO MPD X-ray diffractometer, PANalytical, Almelo, Netherlands) in the 2θ value range of 10-80°. Transmission Electron Microscope (TEM) (FEI Tecnai-G2 30S-TWIN, FEI Company, Hillsboro, OR) was used to study the morphology of the powders. The FTIR analysis of the fillers was performed by PerkinElmer spectrum two IR spectrometer. Shimadzu 3600 UV-vis-NIR spectrophotometer was used for UV-vis absorption spectrum measurement. The morphology of the synthesized fillers and screen printed ink surface was analyzed using Scanning Electron Microscope (SEM) (JEOL, JSM-5600LV, Tokyo, Japan). The colloidal stability of the ink was measured using rheometer (Brookfield, R/S Plus, Massachusetts, USA). The photographic images of the screen printed pattern were recorded with digital camera (Sony, 10x optical zoom, 16M Pixel) and optical images by optical microscopy (Leica, MRDX). The adhesion strength of the screen printed layer on BoPET substrate was measured by using scotch tape analysis recommended by ASTM Standard D3359-02 (Method B), as a standard test method for measuring adhesion. The adhesion test was carried out on freshly printed patterns after 5, 10 and 15 minutes after printing using a Wonder 555^{TM} self-adhesive tape. The EMI shielding measurements were performed using vector network analyzer (Agilent Technologies E5071C, ENA series, 300 kHz-20 GHz, CA) by waveguide method. The sample dimensions used were 22.86 × 10.8 mm for X band (8.2-12.4 GHz) and 15.80 × 7.90 mm for Ku band (12.4-18 GHz) frequency range. For EMI shielding measurements, polyaniline nanofiber and its composite were pressed into sample of thickness 1 mm. The EMI shielding properties of screen printed layers were analyzed by cutting the printed ink on BoPET substrate into required dimensions. The DC conductivity of the polyaniline nanofiber and its composite were measured using four probe method from the current and voltage relationships with current source Aplab 9710 P and nano voltmeter Keithley 2182 A using the same samples used for X band shielding measurements.

3. Results and discussion

3.1 Properties of P and GpP composite

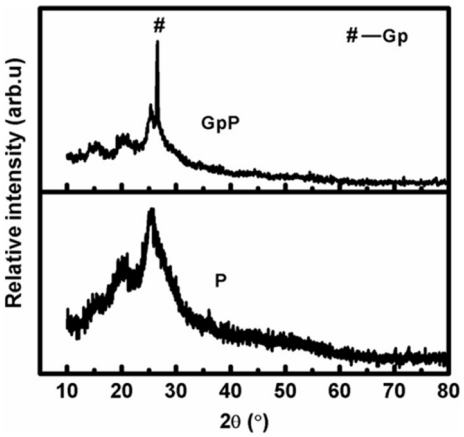

Figure 2 XRD of P and GpP composite.

A very careful balance of ink formulation is required to meet the requirements of the printing process as well as to obtain ink with desired properties. The properties are mainly controlled by the ingredients used in the ink formulation such as filler, solvent, dispersant and binder. The polyaniline nanofiber (P) and polyaniline nanofiber-graphite (GpP) composite are used as the filler in the preparation of screen printing ink. X-ray diffraction patterns (XRD) were recorded to characterize the synthesized P and GpP composite as shown in Figure 2. The diffraction peaks at 2θ values of 15°, 20° and 25° in the XRD pattern of P indicate that the resulting polymer has good crystallinity.[33] The peaks around 2θ = 20° and 25° can be attributed to the periodicity parallel and perpendicular to the polymer chain respectively. The peak at 2θ = 25° indicates that the synthesized P is in the form of highly doped emeraldine salt which is a metallic conductive phase.[34] The XRD pattern of GpP composite has an additional peak at 2θ=26.5° and is attributed to the Gp phases from (002)

reflection.[24] Hence it is clear that both the characteristic peaks of P and Gp appear in the XRD pattern of the GpP composite.

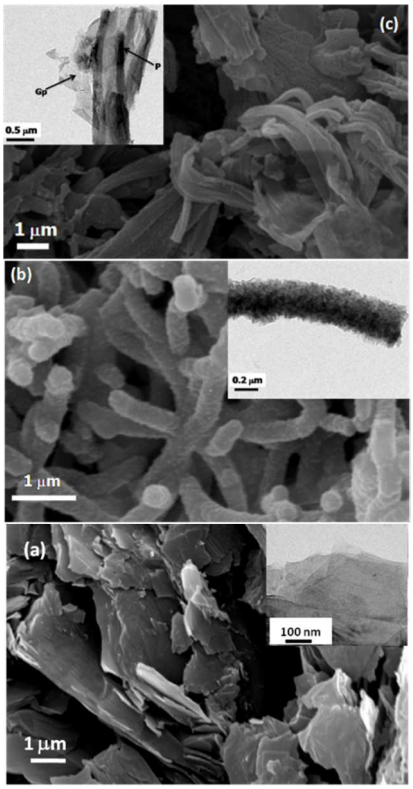

Figure 3 SEM and TEM images of (a) Gp (b) P and (c) GpP composite.

The morphology of graphite flakes (Gp), P and GpP composite are shown in the SEM and TEM images in Figure 3. The SEM (Figure 3 (a)) and TEM (inset of Figure 3 (a)) images of graphite particles clearly demonstrate the uniformly distributed flake like morphology of graphite of few nanometre thickness. It is clear from the SEM image (Figure 3 (b)) that the polyaniline nano fibers have fibrillar morphology with an average diameter of 200 nm. This is more evident from the TEM image of polyaniline nanofiber as given as inset figure of Figure 3 (b). The SEM image of GpP composite as shown in Figure 3 (c) reveals that flake shaped graphite is distributed in the P matrix. The distribution is obvious from the TEM image of the GpP composite (inset figure of Figure 3 (c)). It may be noted that smaller filler particles have an additional advantage since it provides better colloidal stability, dispersion and flow characteristics.[35] It is clear from the SEM as well as TEM images that the addition of graphite has no influence on the morphology of the polyaniline nanofiber. This is due to the presence of only small amount of graphite (2.3 wt.%) in the polyaniline nanofiber-graphite composite (aniline monomer to graphite molar ratio is only 4:1). It is also clear from the FTIR and UV-Visible spectra of P and GpP composite given in Figure 4 and 5 respectively.

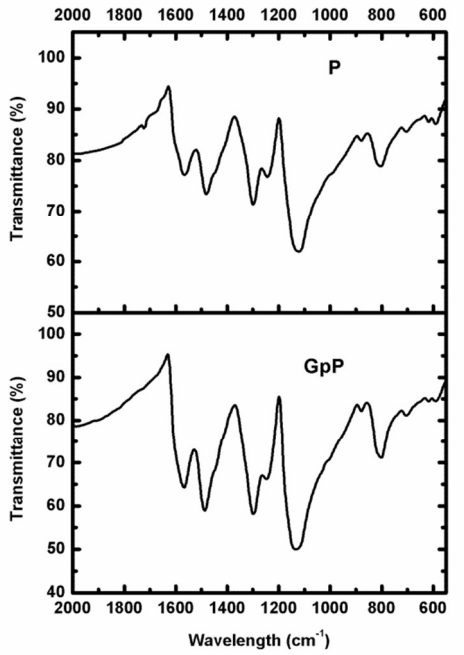

Figure 4 FTIR spectra of P and GpP composite.

The characteristic stretching bands of the quinoid and benzenoid rings of the polyaniline are observed around 1560 cm^{-1} and 1490 cm^{-1} respectively in the FTIR spectra and it represents the conducting state of the polyaniline nanofiber. The absorption peak at 1300 cm^{-1} are attributed to the C-N stretching mode of benzenoid ring and that at 804 cm^{-1} is associated with the C-H out of plane bending modes which indicate the formation of emaraldine salt of polyaniline. The band at 1240 cm^{-1} characterize the conducting protonated polyaniline and corresponds to π electron delocalization induced in the polymer by protonation. The strong peak observed at 1120 cm^{-1} is related to vibration modes of N=Q=N (Q refers to quinonic type rings) in polyaniline nanofiber. This band has been related to the high degree of electron delocalization in polyaniline nanofiber which indicate the formation of conducting polyaniline. The FTIR spectra of GpP composite are similar to that of P which indicate that the synthesized polyaniline nanofiber is in emeraldine salt form. A slight shifting in the absorption peak at 1120 cm^{-1} is observed to 1130 cm^{-1} and this may be due to the interaction between graphite flakes and quinoid rings of polyaniline nanofiber. However, the FTIR spectrum of GpP does not show any new vibration bands indicating that interactions are purely physical in nature. The data obtained agrees well with the published results. [27,36,37,32]

The solid state absorption spectra of P and GpP composite shown in figure 5 has the characteristic peaks of emaraldine salt of polyaniline. It has two bands corresponding to the π-π* transition within the benzenoid segment and n−π* transitions within the quinoid structure. These bands indicate the presence of localized polaronic states such that the synthesized polyaniline nanofiber is in doped form.[32] The bands of the UV-Vis spectra of GpP show only a slight shift and may be due to the increased charge

delocalization over the polymeric backbone on addition of graphite.[37] This may be due to the formation of a charge transfer complex between the doped polyaniline nanofiber and graphite which leads to the good conductivity of the composite as evident from the Table 1. This eventually results in the high EMI shielding efficiency of the GpP composite. The addition of graphite only influences the conductivity and hence the EMI shielding property of the polyaniline nanofiber. In addition to the structural and morphological properties, the EMI shielding properties of the fillers is very important as it is the main factor which determines the shielding response of the final printed patterns.

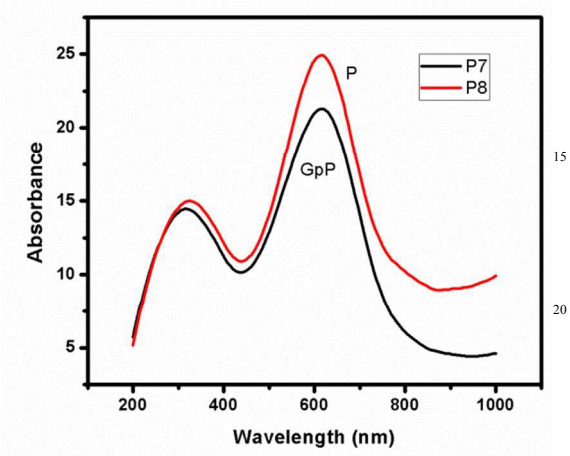

Figure 5 Solid state UV-vis spectra of P and GpP composite.

EMI shielding requires high transmission of the incident EM wave with minimum reflection and the attenuation of the transmitted EM wave by the shielding material. Return loss (RT) is the measure of amount of electromagnetic energy reflected by the material when a sample is inserted in the transmission line.[1] It is given as

$$RT = -20 \log S11 \quad (1)$$

The EMI shielding response can be determined by measuring the EMI shielding effectiveness (EMI SE). It can be obtained from the sum of the net shielding by reflection (reflection shielding effectiveness (SE_R)) and net shielding by absorption (reflection shielding effectiveness (SE_A)). They can be calculated from the magnitude of the experimental scattering parameters S_{11} and S_{12} and are given as [38, 39]

$$\text{EMI SE} = SE_R + SE_A \quad (2)$$

$$SE_R\ (dB) = -10 \log (1 - S_{11}^2) \quad (3)$$

$$SE_A\ (dB) = -10 \log [(S_{21}^2)/ (1 - S_{11}^2)] \quad (4)$$

Table 1 EMI shielding properties and conductivity of polyaniline nanofiber and polyaniline nanofiber-graphite composite.

Material	Average EMI shielding properties in the 8.2-18 GHz frequency range (dB)				DC conductivity (S/cm)
	RT	EMI SE	SE_R	SE_A	
P	0.32	74	12	62	18.5
GpP	0.13	87	16	71	24.0

The return loss, conductivity and EMI shielding efficiency of P and GpP composite with a sample thickness of 1 mm are given in Table 1. It is found that P and GpP exhibit low return loss values of 0.32 and 0.13 dB respectively which indicate maximum transmission of electromagnetic waves into the sample under test. This transmitted electromagnetic waves are attenuated effectively by absorption owing to the good conducting nature of the samples.[31] This is evident from the EMI SE and conductivity values of P and GpP. The polyaniline nanofiber exhibit a conductivity of 18.5 S/cm due to its doped form and is clear from the XRD, FTIR and UV-Vis spectra. It is the emaraldine salt form of polyaniline with indicate the presence of polaronic concentration and are responsible for the good conductivity of polyaniline nanofiber. Addition of graphite flakes into polyaniline nanofiber matrix improves the conductivity to 24.0 S/cm for GpP composite. This slight increase in conductivity is due to the presence of small amount of highly conducting graphite in the polyaniline nanofiber matrix. Graphite is reported to have conductivity of around 10^4 S/cm. The amount of graphite is only 2.3 wt.% in the polymer matrix. The graphite flakes facilitates efficient charge flow through the polymer matrix which results in the improvement in the conductivity. It act as a stable and underlying conductive network to the polyaniline nanofiber. The conductivity of P and GpP composite influences their EMI shielding properties as evident from Table 1. The average EMI SE_R, SE_A and SE of P are 12, 62 and 74 dB respectively in the 8.2-18 GHz frequency range. Polyaniline nanofiber shield the electromagnetic radiation by absorption due to the effective interaction of polarons with the incident electromagnetic radiation.[32] The optimized fibrillar morphology of polyaniline nanofiber with diameter around 200 nm is also responsible for its good conductivity and EMI shielding. [32] The presence of graphite also improves the absorption shielding as well as total EMI SE of polyaniline nanofiber and is clear from the Table 1. The GpP composite has SE_R and SE_A of 16 and 71 dB contributing to the EMI SE of 87 dB in the measured frequency range. The conductivity as well as flake like morphology of the graphite are responsible for the absorption dominated good shielding properties of GpP composite. Effective charge transfer occur between graphite and polyaniline nanofiber due to their conducting nature which in turn results in good absorption shielding. Conductivity and connectivity are important requirements for good EMI shielding.[1] Conducting polyaniline nanofiber and graphite with fibrillar and flake like morphology

respectively provide these features to P and GpP composite which also influences its absorption dominated high EMI shielding efficiency. In addition to this, the morphology and smaller particle size of the order of few nanometres of P and Gp cause multiple reflections of electromagnetic waves within the filler particles. This eventually leads to the high absorption loss of electromagnetic energy due to the increase in the propagation path. Hence energy is dissipated due to the interaction of microwaves with materials causing molecular motions.[31,40-42] The absorption dominated EMI shielding mechanism of P and GpP also depends on the millimeter range of sample thickness (sample thickness is 1 mm) and measurement frequency of GHz.[31,36] Hence the P and GpP composite will prevent nearly 100 % of electromagnetic interference which is excellent for many practical EMI shielding applications. A comparison of the EMI shielding properties of different polyaniline based composites reported in the literature are given in Table 2.

Table 2 EMI shielding effectiveness of polyaniline composites in the X band or Ku band frequency ranges.

Material	Thickness (mm)	EMI SE (dB)	Frequency range (GHz)	Ref
Polyaniline- γ-Fe_2O_3 - graphene oxide core–shell tubes	2.5	51	X band	[42]
Polyaniline-barium strontium titanate-expanded graphite	2.5	81	Ku band	[43]
Polyaniline- graphene -MWCNTs	2.5	98	Ku band	[44]
Polyaniline synthesized by dodecyl benzene sulfonic acid	2.7	55	Ku band	[45]
Polyaniline- Graphene-Fe_3O_4	2.5	29	Ku band	[46]
Polyaniline- $Mn_{0.5}Zn_{0.5}Fe_2O_4$	2	36	X band	[37]
Polyaniline-polystyrene- MWCNTs	2	45	Ku band	[47]
Polyaniline-cobalt ferrite	-	25	Ku band	[48]
Polyaniline -nano-$Mn_{0.2}Ni_{0.4}Zn_{0.4}Fe_2O_4$ ferrite	2.5	49	Ku band	[49]
Polyaniline-MWCNT	2	39	Ku band	[50]
Polyaniline-colloidal graphite	2	40	X band	[51]
Polyaniline-graphite	2	34	X band	[52]
Polyaniline–TiO_2–Fe_2O_3	2	45	Ku band	[53]
Polyaniline-γ-Fe_2O_3	-	11	X band	[54]
Polyaniline nanofiber	1	71-77	X & Ku band	Present work, [32]
Polyaniline nanofiber-graphite composite	1	83-89	X & Ku band	Present work

The EMI SE of the polyaniline nanofiber and polyaniline nanofiber-graphite composite in the present work is much better as compared to the previously reported polyaniline based composites for a lower sample thickness of 1 mm. Moreover polyaniline nanofiber and polyaniline nanofiber-graphite composite with good properties can be easily synthesized by in situ polymerization route without any external agents and solvents. All these results indicate that P and GpP composite can prove to be good candidates for formulating absorbing ink for various EMI shielding applications.

3.2 Ink formulation

Toluene is chosen as the solvent for formulating polyaniline nanofiber based ink. Sodium dodecyl benzene sulfonate (SDBS) is a surfactant and is used as the dispersant in the ink formulation. The main purpose of SDBS addition is to reduce the coagulation of the ink. It will effectively disperse the filler particles in the solvent vehicle and enhance the colloidal stability of the ink. The solvent as well as dispersant are chosen to achieve good screen printability of the ink without much affecting its conductivity. The solvents impart fluidity and act as a vehicle for the uniform distribution of filler particles. Solvents also dissolve the dispersant which is essential to obtain ink with better filler dispersion and thereby the colloidal stability. It also determines the drying rate of the developed ink. Thus the chosen solvent toluene, provides faster drying rate as compared to water based screen printing ink because of its volatile nature. Hence the ink provide room temperature curing effect to the polyaniline nanofiber based ink.

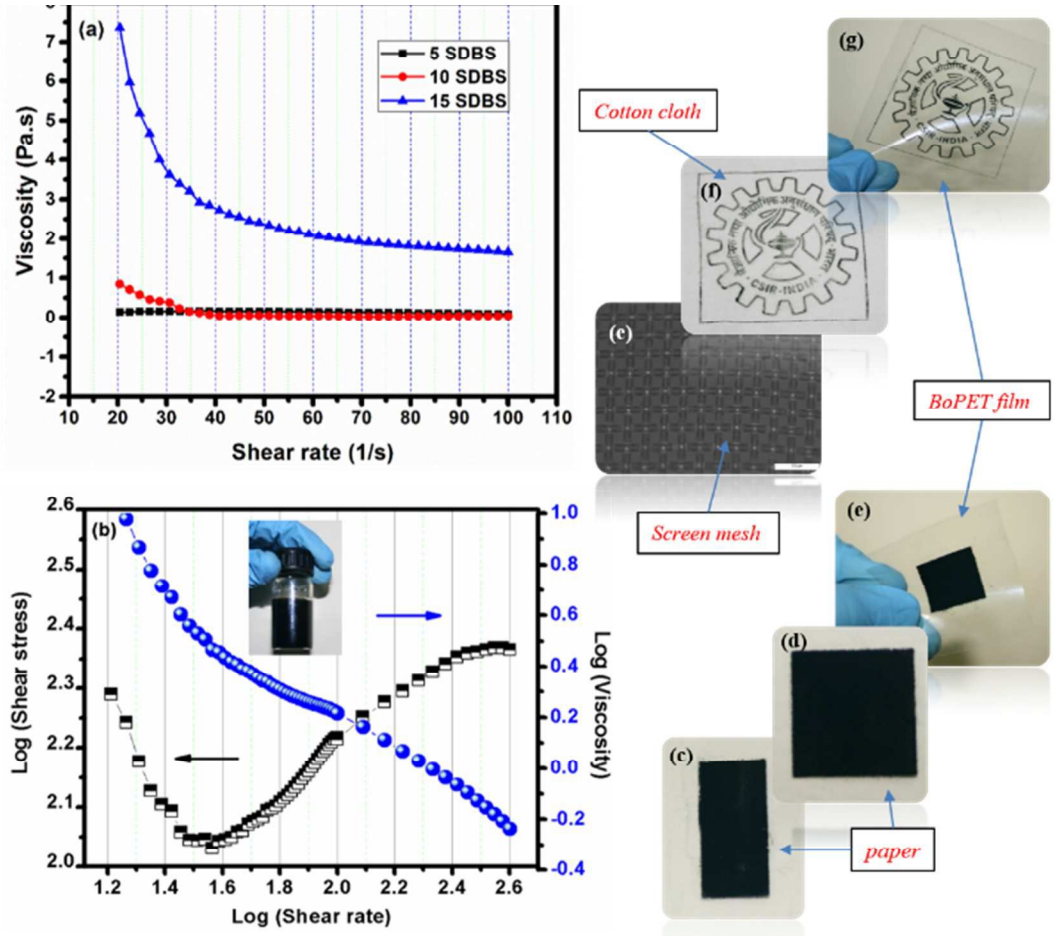

Figure 6 (a) Optimization of the dispersant for ink formulation, (b) final ink rheology, (c) screen printing mesh and photographic images of screen printed polyaniline nanofiber layers on (d, e) paper substrates, (f) cotton cloth and (g, h) BoPET substrate.

The dispersant optimization was performed by keeping the filler loading fixed and gradually varying the dispersant concentration with respect to the filler loading. Figure 6 (a) depicts the viscosity variation of the colloidal mixture as a function of shear rate for different dispersant loading. It is found that the viscosity of colloidal mixture shows a decreasing tendency with increase in shear rate and maintains a pseudoplastic behaviour for 15 wt. % of SDBS. It exhibit an optimal viscosity of around 7 Pa.s at 20 1/s shear rate which is in the range required for screen printing inks.[55-58] The final ink composition consists of toluene as the solvent, 80 wt. % of the filler with respect to solvent and 15 wt. % of surfactant SDBS with respect to filler. The rheology of the final ink composition shown in Figure 6 (b) indicates that with increase in shear rate, shear stress increases while viscosity decreases. Figure 6 (c) represents optical image of the screen printing mesh. Screen printed polyaniline nanofiber layer on various substrates are depicted in the photographic images (Figure 6 (d-h). In the present case screen printed polyaniline nanofiber layer cures in less than 10 minutes depending on the atmospheric conditions.

3.3 Properties of screen printed layer on BoPET film

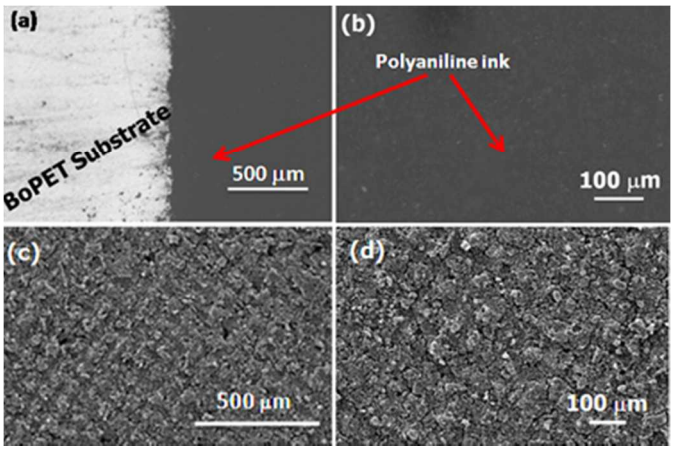

Figure 7 Optical images (a) & (b) and SEM images (c) & (d) of screen printed polyaniline nanofiber layer.

Screen fixing and squeegee movements are important to obtain good quality print. Print quality of screen printed polyaniline

nanofiber layer is also investigated using optical microscopic images and is shown in Figure 7 (a) and (b). A minor spreading of the ink is observed and may be due to the varying squeegee movement during the flood stroke of the printing. It is clear from the optical images that the screen printed polyaniline nanofiber layer on BoPET substrate is of good quality. There is no distorted printing or mesh openings visible in the printed layer and has only thickness of 50 µm. The SEM images of the screen printed surface of polyaniline nanofiber layer given in Figure 7 (c) and (d) present uniformly distributed polyaniline nanofiber. The presence of porosity may be due to the evaporation of organic solvents used in the ink preparation. Ink based on GpP composite also has same surface properties since only a small amount of conductive filler (Gp) is added to obtain polyaniline nanofiber composite. Thus the polyaniline nanofiber ink and polyaniline nanofiber composite ink have same formulation. The polyaniline nanofiber ink screen printed on BoPET substrate is designated as PI and polyaniline-graphite composite ink as GpPI. The scotch test analysis was performed on freshly printed patterns 5, 10 and 15 minutes after printing. The scotch tape test qualitatively confirmed that the screen printed polyaniline nanofiber layer shows good adhesion to the BoPET film even for a single print.

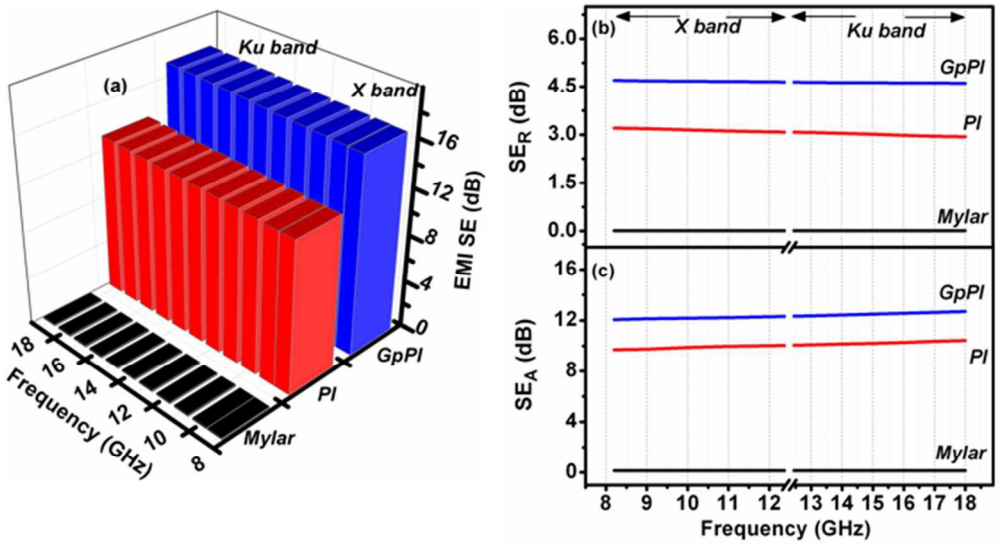

Figure 8 (a) EMI SE (b) SE_R and (c) SE_A of screen printed polyaniline nanofiber based layer in the frequency range of 8.2-18 GHz.

The variation of EMI SE, SE_R and SE_A of polyaniline nanofiber based layer screen printed on BoPET substrate in the frequency range of 8.2-18 GHz are shown in the Figure 8 (a), (b) and (c) respectively. The BoPET substrate has EMI SE of 0.1 dB which indicate that it is transparent to this electromagnetic radiation. Hence it only acts as a substrate to hold the ink with no contribution to the EMI SE. The screen printed polyaniline nanofiber layer has significant EMI SE of above 13 dB resulting in attenuation of above 95% even at a small thickness of 50 µm. The GpPI has EMI SE of 17 dB equal to attenuation of about 98% while that of PI has EMI SE 13 dB in the measured frequency range which is fairly good at this low thickness value.[21] This can be attributed to the good conductivity and EMI shielding properties of P and GpP composite in this frequency range (Table 1).

The EMI SE of these printed patterns has a frequency independent behaviour and hence they provide wide band EMI shielding inks suitable for electrostatic discharge shielding applications. EMI SE less than 20 dB is considered suitable for ESD applications.[59] The mechanism of shielding of these inks can be understood from the contribution of SE_R and SE_A to the EMI SE. The frequency dependence of SE_R and SE_A of screen printed polyaniline nanofiber based layer in the X and Ku band frequency ranges are shown in Figure 8 (b) and (c) respectively. In the measured frequency range, it is observed that for PI, the values of SE_R is 3 dB and SE_A is 10 dB while the value of corresponding parameters for GpPI is 5, 12 dB respectively. These results suggest that the dominant shielding mechanism of these printed layers is absorption in the frequency range of 8.2-18 GHz. This can be attributed to the absorbing shielding property of polyaniline nanofiber. Similar to the EMI SE, GpPI has higher SE_R and SE_A values owing to its slightly higher conductivity than PI. Both SE_R and SE_A of these printed layers are stable with frequency over the wide frequency range of 8.2-18 GHz. These results indicate that the screen printing method can fabricate low cost and flexible EMI shields with little material wastage. In addition to this, EMI shielding of about 20 dB required for commercial EMI applications can be easily prepared by increasing the thickness of printed layer above 50 µm i.e., 100 µm thick printed pattern can provide the required EMI shielding without affecting the flexibility. Thus room temperature curable screen printed absorbing ink based on polyaniline nanofiber with good EMI shielding properties have been developed and hence

are recommended for EMI shielding applications at micrometer scale. Moreover, fillers used in the ink formulation can be easily prepared at room temperature without any external generating agents.

Conclusions

Screen printable inks based on polyaniline nanofiber and its composite were developed for EMI shielding applications. The fillers used in the ink formulation are polyaniline nanofibers and graphite incorporated polyaniline nanofiber composite. These fillers exhibit average EMI SE of 74 and 87 dB respectively in the 8.2-18 GHz frequency range for sample thickness of 1 mm which correspond to an attenuation of 100%. The fillers were synthesized by simple polymerization route. It was observed that the screen printed polyaniline nanofiber based layers exhibit good EMI shielding of above 13 dB (attenuation of above 95%) in the measured frequency range of 8.2-18 GHz at a very small thickness of 50 µm. The dominant shielding mechanism of the polyaniline nanofibers based screen printed layer was absorption. Highest EMI SE of 17 dB was observed for polyaniline nanofiber-graphite based printed layer with SE_R and SE_A of 5 and 12 dB respectively for a thickness of 50 µm. In addition to the good EMI shielding properties, the developed absorbing inks have the advantage of faster curing time and ease of synthesis. The results reveal that efficient EMI shielding materials can be fabricated by simple and low cost screen printing technique. The screen printed polyaniline nanofiber based layer can prove to be a potential absorbing shielding material to meet the commercial EMI shielding demands such as electrostatic discharge etc.

Acknowledgements

Authors are thankful to Mr. M. R. Chandran and Mr. Kiran Mohan for SEM and HRTEM.

Notes and References

a.Materials Science & Technology Division, CSIR NIIST, Thiruvananthapuram 695019, India
b.Microelectronics and Materials Physics Laboratory, P.O. Box 4500, FI-90014, University of Oulu, Finland.
*Corresponding Author: Mailadil Thomas Sebastian, Email Id: mailadils@yahoo.com

[1] N. Joseph, S. K. Singh, R. K. Sirugudu, V. R. K. Murthy, S. Ananthakumar, M. T. Sebastian, Effect of Silver Incorporation into PVDF-Barium Titanate Composites for EMI Shielding Applications, *Mater. Res. Bull*., 2013, **48**, 1681-1687.

[2] D. A. Weston, *Electromagnetic Compatibility: Principles and Applications*, Marcel Dekker, New York, 2001**.**

[3] J. E. Vinson, J. J. Liou, Electrostatic Discharge in Semiconductor Devices: An Overview, *Proc. IEEE*, 1998, **86**, 399-418.

[4] Y. Yang, M. C. Gupta, K. L. Dudley, R. W. Lawrence, Novel Carbon Nanotube-Polystyrene Foam Composites for Electromagnetic Interference Shielding, *Nano Lett.,* 2005, **5**, 2131-2134.

[5] Z. P. Chen, C. Xu, C. Q. Ma, W. C. Ren, H. M. Cheng, Lightweight and Flexible Graphene Foam Composites for High-Performance Electromagnetic Interference Shielding, *Adv. Mater.,* 2013, **25**, 1296-1300.

[6] W. L. Song, Cao,; Lu, M. M.; Bi, S.; Wang, C. Y.; Liu, J.; Yuan, J.; Fan, L. Z.; Flexible Graphene/Polymer Composite Films in Sandwich Structures for Effective Electromagnetic Interference Shielding, *Carbon*, 2014, **66**, 67-76.

[7] T. Mäkelä, T. Haatainen, P. Majander, J. Ahopelto, Continuous Roll to Roll Nanoimprinting of Inherently Conducting Polyaniline, *Microelectronic Engineering,* 2007, **84**, 877-879.

[8] T. K. Kololuoma, M. Tuomikoski, T. Makela, J. Heilmann, T. Haring, J. Kallioinen, J. Hagberg, I. Kettunen, H. K. Kopola, Towards roll-to-roll fabrication of electronics, optics, and optoelectronics for smart and intelligent packaging, Proceedings of the SPIE 5363, **2004**, *77* (San Jose, CA, USA).

[9] Chromaline Screen Printing Product Guide, https://www.chromaline.com/printed-electronics/**2015**.

[10] S. Monie, Retrieved from Industrial Specialty Printing website,http://industrial-printing.net/content/developmentsconductive-inks?Page=0%2C3, **2010.**

[11] L. Grande, V. T. Chundi, D. Wei, C. Bower, P. Andrew, T. Ryhänen, Graphene for energy harvesting/storage devices and printed electronics, *Particuology*, 2012, **10**, 1-8.

[12] I. J. Gauscmeier, Thinking Ahead the Future of Additive Manufacturing-Innovation Roadmapping of Required of Required Advancements, *DMRC study Part-3*, University of Paderborn, **2013**, 48-51.

[13] [13] P. Chandrasekhar, *Conducting Polymers, Fundamentals and Applications: A Practical Approach*, Kluwer Academic, Netherlands, **1999**.

[14] P. Saini, V. Choudhary, N. Vijayan, R. K. Kotnala, Improved Electromagnetic Interference Shielding Response of Poly(aniline)-Coated Fabrics Containing Dielectric and Magnetic Nanoparticles, *J. Phys. Chem. C*, 2012, **116**, 13403-13412.

[15] T. A. Skotheim, R. L. Elsenbaumer, J. R. Reynolds, *Handbook of Conducting Polymers*, Marcel Dekker, New York, **1998**.

[16] J. Joo, A. J. Epstein, Electromagnetic Radiation Shielding by Intrinsically Conducting Polymers, *Appl. Phys. Lett.*, 1994, **65**, 2278-2280.

[17] P. Saini, V. Choudhary, S. K. Dhawan, Improved Microwave Absorption and Electrostatic Charge Dissipation Efficiencies of Conducting Polymer Grafted Fabrics Prepared via In-situ Polymerization, *Polym. Adv. Technol*., 2012, **23**, 343-349.

[18] S. Sivaram, *Polymer Science Contemporary Themes*, Tata McGraw-Hill, India **1991**.

[19] M. Aldissi, *Intrinsically Conducting Polymers: An Emerging Technology*, Kluwer Academic, Netherlands **1993.**

[20] T. A. Skotheim, J. R. Reynolds, *Handbook of Conducting Polymers third edition: Conjugated Polymers−Processing and Applications,* CRC Press, United States **2007**.

[21] L. L. Wang, B. K. Tay, K. Y. See, Z. Sun, L. K. Tan, D. Lua, Electromagnetic Interference Shielding Effectiveness of Carbon-Based Materials Prepared by Screen Printing, *Carbon* 2009, **47**, 1905-1910.

[22] D. C. Trivedi, *Handbook of Organic Conductive Molecules and Polymers*, John Wiley & Sons Ltd, United Kingdom **1997**.

[23] M. V. Kulkarni, S. K. Apte,; S. D. Naik, J. D. Ambekar,; B. B. Kale, Ink-jet Printed Conducting Polyaniline Based Flexible Humidity Sensor, *Sensors and Actuators B***,** 2013, **178**, 140-143.

[24] H. Fuan, L. Sienting, L. C. Helen, F. Jintu, High Dielectric Permittivity and Low Percolation Threshold in Nanocomposites Based on Poly(vinylidene fluoride) and Exfoliated Graphite Nanoplates, *Adv.Mater.,* 2009, **21**, 710-715.

[25] Y. Xu, I. Hennig, D. Freyberg, A. J. Strudwick, M. G. Schwab, T. Weitz, K. C. Pei Cha, Inkjet-Printed Energy Storage Device Using Graphene/Polyaniline Inks, *Journal of Power Sources*, 2014, **248**, 483-488.

[26] I. A. Tchmutin, A. T. Ponomarenko, E. P. Krinichnaya, G. I. Kozub, O. N. Efimov, Electrical Properties of Composites Based on Conjugated Polymers and Conductive Fillers, *Carbon,* 2003, **41**, 1391-1395.

[27] X. S. Du, M. Xiao, Y. Z. Meng, Facile Synthesis of Highly Conductive Polyaniline/graphite Nanocomposites, *Eur. Polym. J.,* 2004, **40**, 1489-1493.

[28] S. E. Bourdo, T. Viswanathan, Graphite/Polyaniline (GP) Composites: Synthesis and Characterization, *Carbon*, 2005, **43**, 2983-2988.

[29] Y. Xu, M. G. Schwab, A. J. Strudwick, I. Hennig, X. Feng, Z. Wu, K. Müllen, Screen-Printable Thin Film Supercapacitor Device Utilizing Graphene/Polyaniline Inks, Adv. Energy Mater., 2013, **3**, 1035–1040.

[30] N.B. Clark, L.J. Maher, Non-contact, radio frequency detection of ammonia with a printed polyaniline sensor, *React. Funct. Polym.*, 2009, **69**, 594–600.

[31] Z. Stempien, T. Rybicki, E. Rybicki, M. Kozanecki, M.I. Szynkowska, In-situ deposition of polyaniline and polypyrrole electroconductive layers on textile surfaces by the reactive ink-jet printing technique, *Synth. Met.*, 2015, **202**, 49-62.

[32] N. Joseph, J. Varghese, M. T. Sebastian, Self-Assembled Polyaniline Nanofibers with Enhanced Electromagnetic Shielding Properties, *RSC Adv.,* 2015, **5**, 20459-20466.

[33] K. Lee, S. Cho, S. H. Park, A. J. Heeger, C. W. Lee, S. H. Lee, Metallic Transport in Polyaniline, *Nature,* 2006, **441**, 65-68.

[34] J. P. Pouget, M. E. Jozefowicz, A. J. Epstein, X. Tang, A. G. MacDiarmid, X-ray Structure of Polyaniline, *Macromolecules,* 1991, **24**, 779-789.

[35] J. T. Kunjappu, *Essays in ink chemistry*, Nova Science Publishers, New York **2001**.

[36] H. R. Tantawy, D. E. Aston, J. R. Smith, J. L. Young, Comparison of Electromagnetic Shielding with Polyaniline Nanopowders Produced in Solvent-Limited Conditions, *ACS Appl. Mater. Interfaces,* 2013, **5**, 4648-4658.

[37] M. Abdullah Dar, R. K. Kotnala, V. Verma, J. Shah, W. A. Siddiqui, M. Alam, High Magneto-Crystalline Anisotropic Core-Shell Structured $Mn_{0.5}Zn_{0.5}Fe_2O_4$/Polyaniline Nanocomposites Prepared by in Situ Emulsion Polymerization, *J. Phys. Chem. C*, 2012, **116**, 5277-5287.

[38] D. Annapurna, K. D. Sisir, *Microwave Engineering*, Tata McGraw Hill, India **2009**.

[39] N. Joseph, M. T. Sebastian, Electromagnetic Interference Shielding Nature of PVDF-Carbonyl Iron Composites, *Mater. Lett.*, 2013, **90**, 64-67.

[40] S. W. Guang, J. Z. Xiao, Z. W. Yun, H. Shuai, G. Lin, S. C. Mao, Polymer Composites with Enhanced Wave Absorption Properties Based on Modified Graphite and Polyvinylidene Fluoride, *J. Mater. Chem. A*, 2013, **1**, 7031-7036.

[41] C. Zongping, X. Chuan, M. Chaoqun, R. Wencai, M. C. Hui, Lightweight and Flexible Graphene Foam Composites for High-Performance Electromagnetic Interference Shielding, *Adv. Mater.,* 2013, **25**, 1296-1300.

[42] A. P. Singh, M. Mishra, P. Sambyal, B. K. Gupta, B. P. Singh, A. Chandrad, S. K. Dhawan, Encapsulation of γ-Fe_2O_3 Decorated Reduced Graphene Oxide in Polyaniline Core–shell Tubes as an Exceptional Tracker for Electromagnetic Environmental Pollution, *J. Mater. Chem. A*, 2014, **2**, 3581-3593.

[43] P. Sambyal, A. P. Singh, M. Verma, M. Farukh, B. P. Singh, S. K. Dhawan, Tailored polyaniline/barium strontium titanate/expanded graphite multiphase composite for efficient radar absorption, *RSC Adv.* 2014, **4**, 12614-12624.

[44] T. K. Gupta, B. P. Singh, R. B. Mathur, S. R. Dhakate, Multi-walled Carbon Nanotube–Graphene–Polyaniline Multiphase Nanocomposite with Superior Electromagnetic Shielding Effectiveness, *Nanoscale*, 2014, **6**, 842-851.

[45] P. Saini, M. Arora, Formation Mechanism, Electronic Properties & Microwave Shielding by Nano-Structured Polyanilines Prepared by Template Free Route Using Surfactant Dopants, *J. Mater. Chem. A*, 2013, **1**, 8926-8934.

[46] K. Singh, A. Ohlan, V. H. Pham, R. Balasubramaniyan, S. Varshney, J. Jang, S. H. Hur, W. M. Choi, M. Kumar, S. K. Dhawan, B. S. Kong, J. S. Chung, Nanostructured Graphene/Fe_3O_4 Incorporated Polyaniline as a High Performance Shield Against Electromagnetic Pollution, *Nanoscale*, 2013, **5**, 2411-2420.

[47] P. Saini, V. Choudhary, R. Singh, B. Mathur, S. K. Dhawan, Enhanced Microwave Absorption Behavior of

Polyaniline-CNT/polystyrene Blend in 12.4–18.0 GHz Range, *Synth. Met.,* 2011, **161**, 1522-1526.

[48] N. K. Gandhi, B. P. Singh, A. Ohlan, D. P. Singh, S. K. Dhawan, Thermal, Dielectric and Microwave Absorption Properties of Polyaniline–$CoFe_2O_4$ Nanocomposites, *Compos. Sci. Technol.,* 2011, **71**, 1754-1760.

[49] S. P. Gairola, V. Verma, L. Kumar, M. Abdullah Dar, M. Annapoorni, R. K. Kotnala, Enhanced Microwave Absorption Properties in Polyaniline and Nano-Ferrite Composite in X-band, *Synth. Met.*, 2010, **160**, 2315-2318.

[50] P. Saini, V. Choudhary, B. P. Singh, R. B. Mathur, S. K. Dhawan, Polyaniline–MWCNT Nanocomposites for Microwave Absorption and EMI Shielding, *Mater. Chem. Phys.* 2009, **113**, 919-926.

[51] P. Saini, V. Choudhary, S. K. Dhawan, Electrical Properties and EMI Shielding Behavior of Highly Thermally Stable Polyaniline/Colloidal Graphite Composites, *Polym. Adv. Technol.*, 2009, **20**, 355-361.

[52] P. Saini, V. Choudhary, K. N. Sood, S. K. Dhawan, Electromagnetic Interference Shielding Behavior of Polyaniline/Graphite Composites Prepared by *in situ* Emulsion Pathway, *J. Appl. Polym. Sci.*, 2009*,* **113**, 3146-3155.

[53] S. K. Dhawan, K. Singh, A. K. Bakhshi, A. Ohlan, Conducting Polymer Embedded with Nanoferrite and Titanium Dioxide Nanoparticles for Microwave Absorption, *Synth. Met.,* 2009, **159**, 2259-2262.

[54] K. Singh, A. Ohlan, R. K. Kotnala, A. K. Bakhshi, S. K. Dhawan, Dielectric and Magnetic Properties of Conducting Ferromagnetic Composite of Polyaniline with γ-Fe_2O_3 Nanoparticles, *Mater. Chem. Phys*., 2008, **112**, 651-658.

[55] C. A. Harper, *Handbook of Thick* Film Hybrid Microelectronics, McGraw-Hill Book, Company, New York **1974**.

[56] M. Lahti, S. Leppävuori, V. Lantto, Gravure-offset-printing technique for the fabrication of solid films, *Appl. Surf. Sci.* 1999, **142**, 367-370.

[57] J. Varghese, K. P. Surendran, M. T. Sebastian, Room Temperature Curable Silica Ink, *RSC Advances*, 2014, **4**, 47701-47707.

[58] J. Varghese, M. Teirikangas, J. Puustinen, H. Jantunen, M. T. Sebastian, Room Temperature Curable Zirconium Silicate Dielectric Ink for Electronic Applications, *J. Mater. Chem. C*, 2015, **3**, 9240-9246.

[59] N. Joseph, J. Chameswary, M. T. Sebastian, Electromagnetic Interference Shielding Properties of Butyl Rubber-Single Walled Carbon Nanotube Composites, *Compos. Sci. Technol*. 2014, **101**, 139–144.

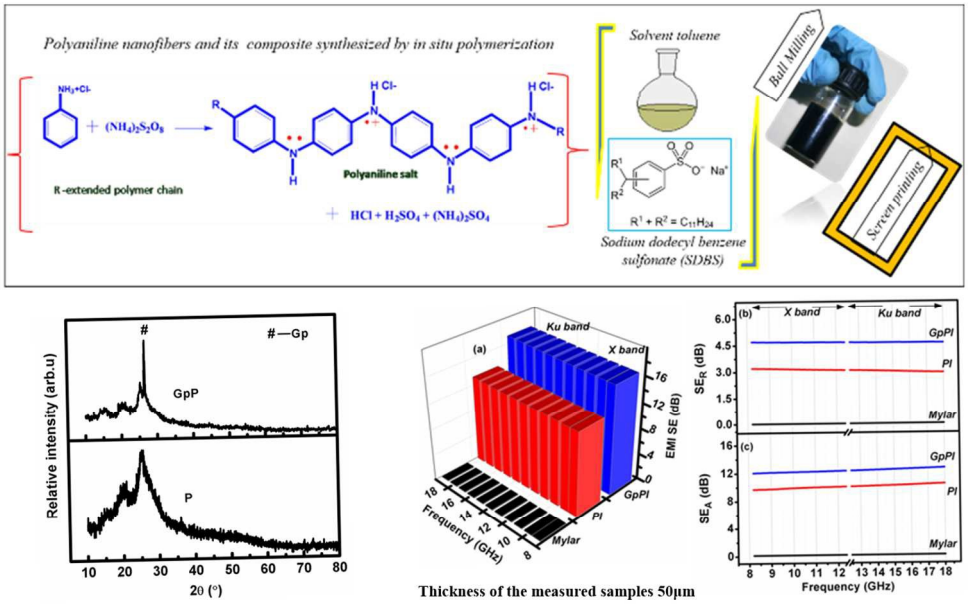

Ultra low thickness EMI shielding ink
247x155mm (150 x 150 DPI)